Electronic Supplementary Information

Carbon Dioxide Capture in the Presence of Water by an Amine-based Crosslinked Porous Polymer

Mahmoud M. Abdelnaby,[1,2] Ahmed M. Alloush,[1,3] Naef A. A. Qasem,[3] Bassem A. Al-Maythalony,[3] Rached B. Mansour,[3] Kyle E. Cordova,[2,4] and Othman Charles S. Al-Hamouz*[,1]

[1]Department of Chemistry, King Fahd University of Petroleum and Minerals (KFUPM), Dhahran 31261, Saudi Arabia

[2]Center for Research Excellence in Nanotechnology (CENT), KFUPM, Dhahran, 31261, Saudi Arabia

[3]King Abdulaziz City for Science and Technology—Technology Innovation Center on Carbon Capture and Sequestration (KACST-TIC on CCS), KFUPM, Dhahran 31261, Saudi Arabia

[4]Berkeley Global Science Institute, University of California—Berkeley, Berkeley, California 94720, United States

To whom correspondence should be addressed: othmanc@kfupm.edu.sa

Table of Contents

Section S1: Materials and Methods

Pyrrole (98% purity), 1,4-benzenediamine (DA, 98% purity), methanol (99.9% purity), *N,N*-dimethylformamide (99% purity), and hydrochloric acid (37 wt%) were purchased from Sigma Aldrich Co. Anhydrous iron(III) chloride (≥99.99% purity) was acquired from Alpha Chemika. Paraformaldehyde (≥99% purity) was obtained from Fluka. Ammonium hydroxide (28-30 *w*/*w*%) was purchased from Fisher Scientific. Pyrrole was distilled under N_2 flow at 145 °C and stored under a N_2 environment at -4 °C prior to use. All other chemicals were used without further purification. For gas sorption measurements, ultrahigh purity grade nitrogen (99.999%), helium (99.999%), and high purity CO_2 (99.9%) were obtained from Abdullah Hashem Industrial Co., Dammam, Saudi Arabia.

^{13}C solid state nuclear magnetic resonance (NMR) spectroscopy measurements were performed on a Bruker 400 MHz spectrometer operating at 125.65 MHz (11.74 T) and at ambient temperature (298 K). Samples were packed into 4 mm ZrO_2 rotors and cross-polarization magic angle spinning (CP-MAS) was employed with a pulse delay of 5.0 s and a magic angle spinning rate of 10 kHz for the 1,4-benzenediamine monomer or 14 kHz for the polymer. Fourier transform infrared (FT-IR) spectroscopy measurements were performed from KBr pellets using a PerkinElmer 16 PC spectrometer. The spectra were recorded over 4000 – 400 cm^{-1} in transmission mode and the output signals were described as follows: s, strong; m, medium; w, weak; and br, broad. Thermal gravimetric analysis (TGA) was run on a TA Q-500 instrument with the sample held in a platinum pan under air flow with a 10 °C per min heating rate. To identify the type of gases trapped within the pores, TGA-mass spectrometry (TGA-MS) analysis was performed using a QMS 403 C Aëolos with STA 449 F1 Jupiter instrument. Powder X-ray diffraction (PXRD) measurements were carried out using a Rigaku MiniFlex II X-ray diffractometer with Cu K_α radiation (λ = 1.54178 Å). Field emission scanning electron microscope (FE-SEM) images were taken on a Tescan LYRA3 Dual Beam microscope at an acceleration voltage of 10 kV. Low pressure nitrogen sorption isotherms were collected on a Micromeritics ASAP 2020. A liquid nitrogen bath was used for the measurements at 77 K. CO_2 sorption isotherms were carried out on an Autosorb iQ2 volumetric gas adsorption analyser. The measurement temperatures at 273 and 298 K were controlled with a water circulator. Water adsorption measurements were performed on a DVS Vacuum, Surface Measurement Systems Ltd, London, UK. Prior to these measurements, KFUPM-1 was pre-treated by heating (383 K) under vacuum for 10 hours using the Dynamic Vapor Sorption Analyzer Desorption attachment.

Section S2: Synthetic Procedures

Different parameters were applied in order to synthesizes the KFUPM-1 polymer, in all the trials the monomer 1,4-benzendiamine and pyrrole were used by (1:2) molar ratios respectively.

Table S1. Optimization conditions for KFUPM-1 synthesis.

Condition No.	Linker	Solvent	Catalyst	Catalyst mol %	Temperature (K)	Remarks
1	*p*-formaldehyde dimethyl acetal	1,2-dichloroethane	$FeCl_3$	10[b]	323 -353	Nonporous material
2	*p*-formaldehyde dimethyl acetal	1,2-dichloroethane	$FeCl_3$	100[b]	323 -353	Nonporous material
3	*p*-formaldehyde	DMSO	$FeCl_3$	10[b]	363	Low yield
4	*p*-formaldehyde	DMSO	Conc. HCl	27[a]	363	Low yield
5	*p*-formaldehyde	DMF	Conc. HCl	27[a]	363	Micropore with good CO_2 uptake
6	*p*-formaldehyde	DMF	$FeCl_3$	10[b]	363	Low CO_2 uptake
7	*p*-formaldehyde	DMF	CuCl	10[b]	263	High Cu content in final product

[a]mol % of all the monomers, [b]mol% of linker

Synthesis of model polymer. Paraformaldehyde (0.60 g, 20 mmol) and 1,4-benzenediamine (0.60 g, 5.5 mmol) were added with 20 mL DMF to a 50 mL round bottom flask. This mixture was stirred for 15 min., at which time 0.4 mL conc. HCl (12 M) was added. The round bottom flask was sealed with a rubber septum and heated at 323 K for 15 h and at 363 K for 9 h with a stirring rate of 200 rpm. After this time elapsed, a yellow precipitate was observed and isolated by centrifugation. This solid was then washed with 20 mL of methanol. The yellow product was filtered and washed with 20 mL of methanol per d for 3 d with

continuous stirring. Finally, the product was dried at 348 K under vacuum (<0.1 bar) for 15 h. The final yield (0.65 g) was 77% based on the 1,4-benzenedaimine monomer. FT-IR (KBr, cm^{-1}) 3379 (br), 3217 (w), 2916 (w), 2850 (w), 1651 (s), 1604 (w), 1512 (m), 1385 (w), 1130 (w), 822 (w).

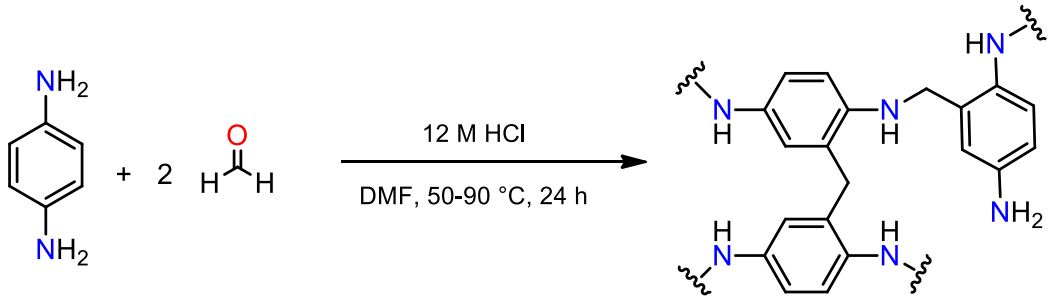

Scheme S1. Synthetic scheme of model polymer.

Synthesis of KFUPM-1. 1,4-Benzenediamine (1.08 g, 10.0 mmol) and paraformaldehyde (1.20 g, 40.0 mmol) were combined with 70 mL DMF to a 100 mL round bottom flask and stirred at room temperature for 5 min. Pyrrole (1.34 g, 20.0 mmol) was then added into the reaction mixture and stirred for an additional 5 min. After this, 1.6 mL conc. HCl (12 M) was added dropwise into the reaction mixture and the flask was sealed with a rubber septum and purged with N_2 for 2-3 min. The mixture was subsequently heated at 363 K in an oil bath for 24 h with continuous stirring at a rate of 200 rpm. After this time elapsed, a black solid was isolated by filtration. The solid was washed with 40 mL of methanol followed by sonication for 30 min. The solid was filtered and immersed in an ammonia solution (25% *w*/*w*) for 24 h, 40 mL distilled water for 24 h, and 60 mL of methanol per d for 3 d with stirring, at which time a clear filtrate solution was obtained. Finally, the product was dried at 348 K under vacuum (<0.1 bar) for 20 h. The final yield (2.56 g) was 88% based on the monomers weights. FT-IR (KBr, cm^{-1}) 3413 (br), 3240 (br), 2918 (w), 2852 (w), 1618 (m), 1510 (w), 1423 (w), 1024 (w), 671 (m).

Exact yield calculation:

% yield = (experimental weight/(total monomers weights-weight of the H_2O)) * 100

= 2.56 / (1.08 + 1.34 + 1.2 – (0.04 mol * 18)) = 2.56/ 2.9 = 88%

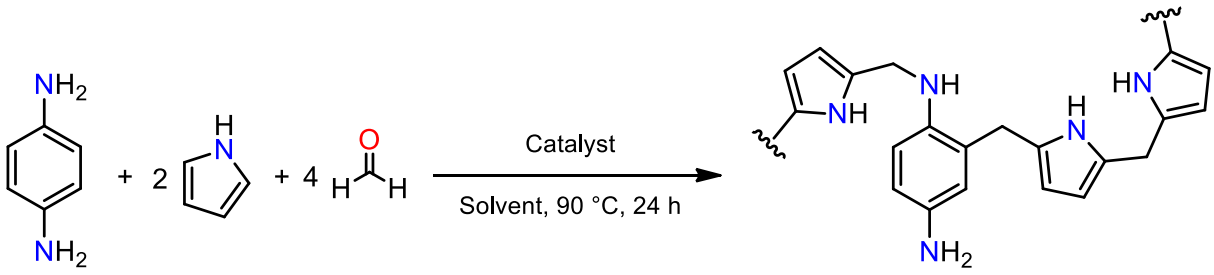

Scheme S2. General synthetic scheme of KFUPM-1 polymer.

Synthesis of KFUPM-1/$FeCl_3$. 1,4-Benzenediamine (0.27 g, 2.5 mmol) and paraformaldehyde (0.30 g, 10 mmol) were added with 20 mL DMF to a 50 mL round bottom flask and stirred at room temperature for 5 min. After this, pyrrole (0.36 g, 5.4 mmol) was added into the reaction mixture and continuously stirred for an additional 5 min. and then the flask was purged with N_2 for 2-3 min and subsequently Iron (III) chloride ($FeCl_3$, 0.16 g, 1 mmol) was added under inert atmosphere and the flask was sealed with a rubber septum. The mixture was heated at 363 K in an oil bath for 24 h with continuous stirring at a rate of 200 rpm. After this time elapsed, a black solid was isolated by centrifugation and filtration. The solid was washed with 40 mL of methanol followed by sonication for 30 min. The solid was filtered and immersed in an ammonia solution (25% *w*/*w*) for 24 h, 40 mL distilled water for 24 h, and 60 mL of methanol per d for 3 d with stirring, at which time a clear filtrate solution was obtained. Finally, the product was dried at 348 K under vacuum (<0.1 bar) for 20 h. The final yield (0.59 g) was 78% based on the monomers weights. FT-IR (KBr, cm^{-1}) 3431 (br), 3267 (br), 2927 (w), 2868 (w), 1612 (w), 1512 (w), 1433 (w), 1120 (w), 673 (m).

Synthesis of KFUPM-1/CuCl. 1,4-Benzenediamine (1.08 g, 10.0 mmol) and paraformaldehyde (1.20 g, 40.0 mmol) were added with 60 mL DMF to 100 mL round bottom flask and stirred at room temperature for 5 min. After this pyrrole (1.34 g, 20.0 mmol) was added into the reaction mixture and continuously stirred for 5 min. and then the flask was purged with N_2 for 2-3 min and subsequently copper (I) chloride (CuCl, 0.39 g, 4.0 mmol) was added under inert atmosphere and the flask was sealed with a rubber septum. The mixture was heated at 363 K in an oil bath for 24 h with continuous stirring at a rate of 200 rpm. After this time elapsed, a black solid was isolated by centrifugation and filtration. The solid was washed with 40 mL of methanol followed by sonication for 30 min. The solid was filtered and immersed in an ammonia solution (25% *w*/*w*) for 24 h, 40 mL distilled water for 24 h, and 60

mL of methanol per d for 3 d with stirring, at which time a clear filtrate solution was obtained. Finally, the product was dried at 348 K under vacuum (<0.1 bar) for 20 h. The final yield (3.00 g) was 100% based on the monomers weights. FT-IR (KBr, cm^{-1}) 3406 (br), 3236 (br), 2920 (w), 2848 (w), 1614 (w), 1510 (w), 1107 (w), 827 (m).

Section S3: Structural Characterization

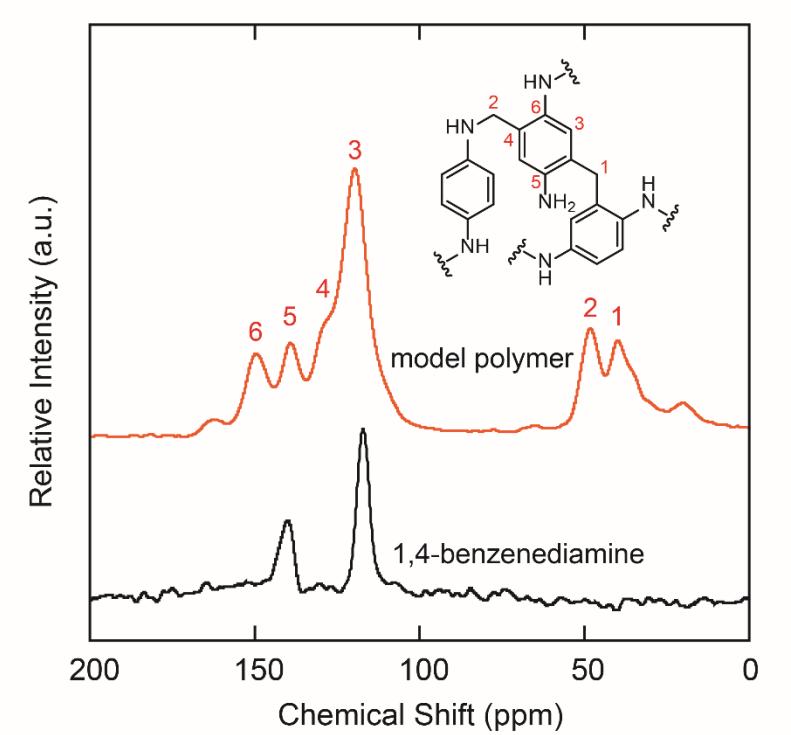

Figure S1. Solid state CP-MAS ^{13}C-NMR stack mode of the model polymer and the 1,4-benzenediamine monomer at 10 KHz with the corresponding core structure of model polymer provided in the inset for peak assignment.

Table S2. Assignment of the ^{13}C NMR spectrum peaks of the model polymer.

Peaks (ppm)	Peak No.	Assignment of the characteristic peaks in the structure
39	1	Aliphatic CH_2 linkage between aromatic C atoms form two phenylene rings
48	2	Aliphatic CH_2 linkage between aromatic C atom NH group of another molecule
119	3	Non-substituted aromatic C
129	4	Substituted aromatic C
138	5	Quaternary carbon attached to free amine group
149	6	Quaternary carbon attached to linked amine group

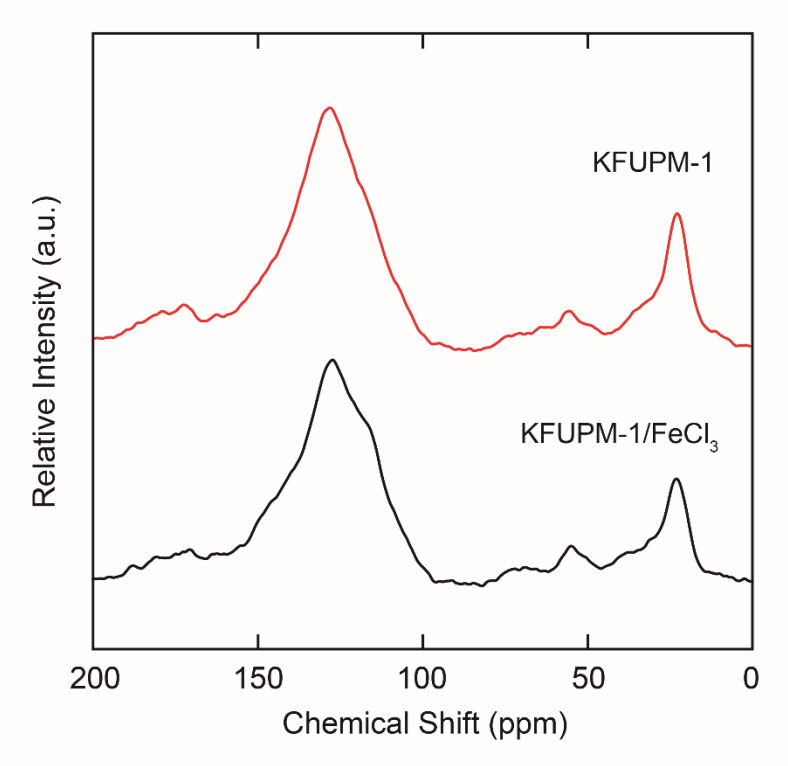

Figure S2. ^{13}C CP-MAS NMR spectra of KFUPM-1 and KFUPM-1/$FeCl_3$ at 14 KHz.

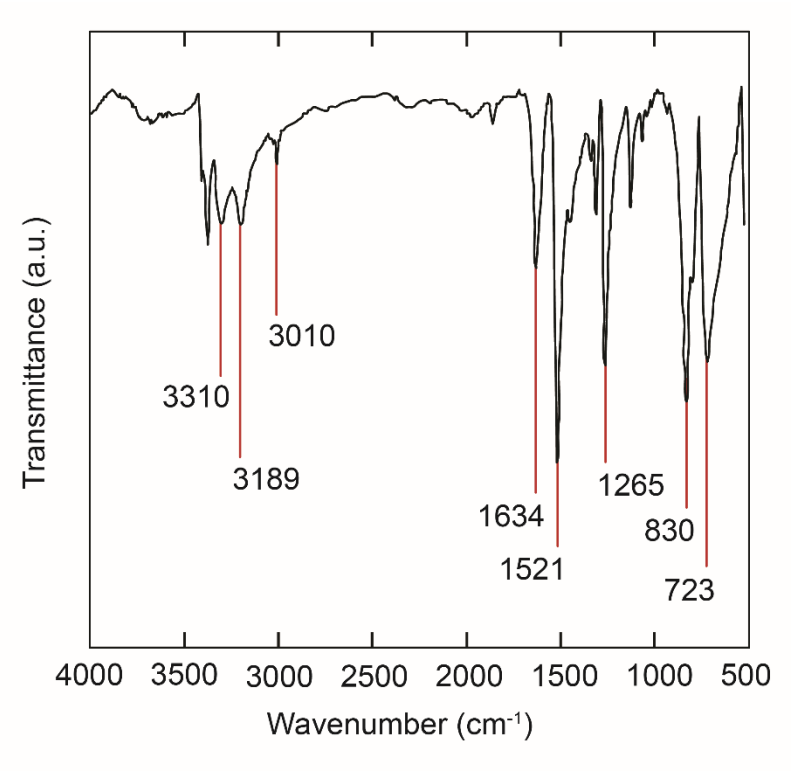

Figure S3. FT-IR spectrum of 1,4-benzenediamine monomer.

Table S3. Assignment of the FT-IR spectrum peaks of the 1,4-benzenediamine monomer.

Band Position (cm^{-1})	Band Assignments & Description
3310 (m) & 3189 (m)	NH_2 stretch (asymmetric, higher frequency, and symmetric)
3010 (w)	Aromatic C—H stretch
1634 (m)	Aromatic C=C vibration mode for aromatic ring
1521 (s)	Phenyl ring C=C vibration mode
1265 (s)	Can be assigned to the C—N stretch
830 (s)	C-H bending
723 (s)	NH_2 wagging

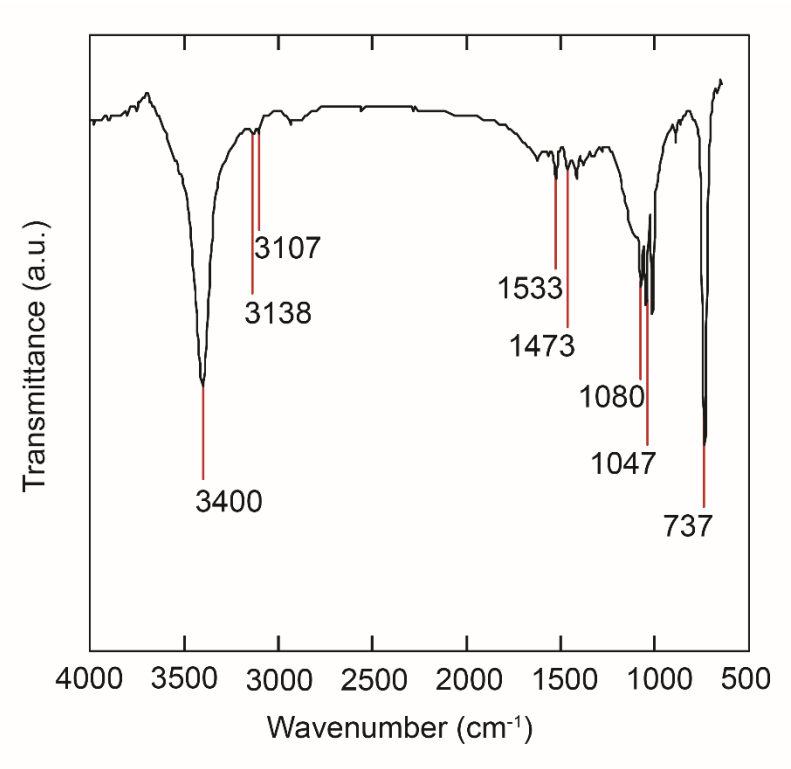

Figure S4. FT-IR spectrum of pyrrole monomer.

Table S4. Assignment of the FT-IR spectrum bands of the pyrrole monomer.

Band Position (cm^{-1})	Band Assignments & Notes
3400 (s)	NH stretching from the pyrrole ring
3138 (w)	Aromatic =C-H stretching from the pyrrole ring
3107 (w)	Aromatic =C-H stretching from the pyrrole ring
1533 (w)	Aromatic ring stretching
1473 (w)	Aromatic ring stretching
1080 (m)	Aromatic C-H bending
1047 (m)	Aromatic C-H bending
737 (s)	NH wagging (H-bonded)

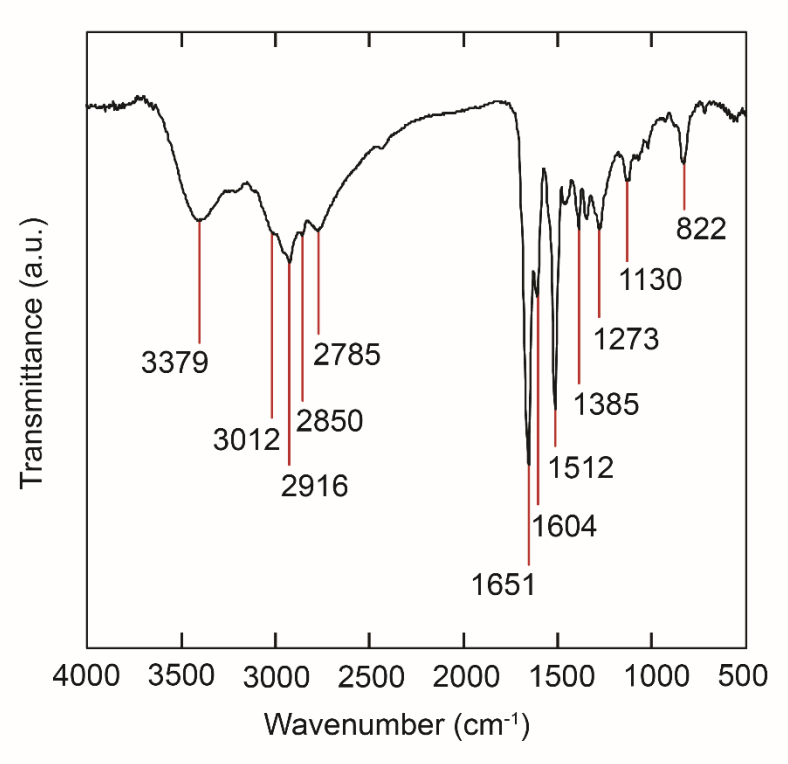

Figure S5. FT-IR spectrum of model polymer.

Table S5. Assignment of the FT-IR spectrum bands of the synthesized model polymer.

Band Position (cm^{-1})	Band Assignments & Description
3379 (br)	2ry amine N-H stretching, is considered as an evidence for the methylene linkage from the formaldehyde at the NH_2
3012 (w) & 2916 (w)	Aromatic C-H stretching from the phenyl ring
2850 (w)	Methylene C-H stretch specific for CH_2 linkage for the polymer NOT present in the benzenediamine ring
1651 (s)	Aromatic C=C vibration mode
1512 (s)	Phenyl ring C=C vibration mode
1385 (m)	Can be assigned CH_2 deformation band
1130 (w)	C-N stretching
822 (w)	NH_2 wagging

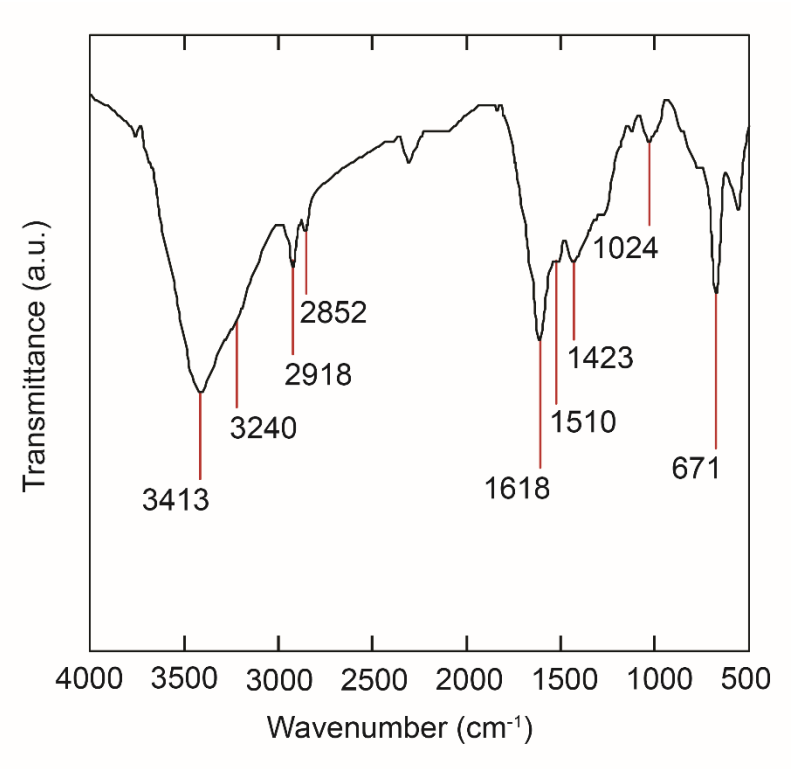

Figure S6. FT-IR spectrum of KFUPM-1

Table S6. Assignment of the FT-IR spectrum bands of the synthesized KFUPM-1.

Band Position (cm^{-1})	Band Assignments & Description
3413 (br)	N-H stretch from both pyrrole & benzenediamine moieties overlap with O-H stretch of terminal groups
3240 (w)	Can be assigned to NH_2 stretches of 1,4-benzenediamine moiety
2918 (w)	Aliphatic C-H stretch of CH_2 linkage, NOT present in neither benzenediamine nor pyrrole monomers
1618 (m)	Aromatic C=C vibration mode for the Asymmetric aromatic rings
1510 (w)	Phenyl ring C=C vibration mode, characteristic band, proves the presence of the benzenediamine moiety in the copolymer
1423 (w)	Can be assigned to the phenyl C=C vibrational mode
1124 (w)	C-N stretch in both benzenediamine & pyrrole moieties
671 (w)	NH_2 wagging

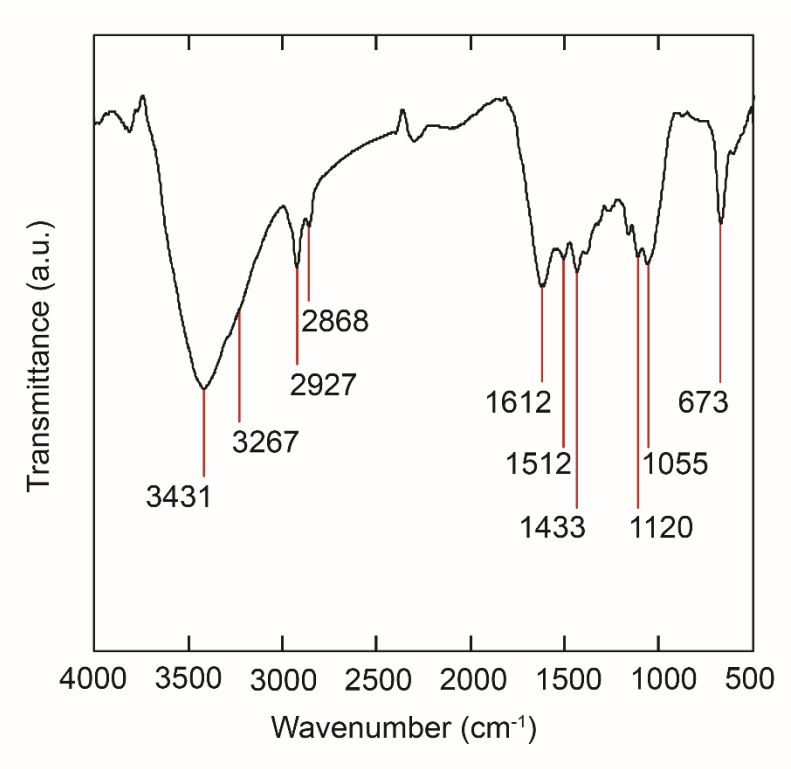

Figure S7. FT-IR spectrum of KFUPM-1/$FeCl_3$.

Table S7. Assignment of the FT-IR spectrum peaks of the synthesized KFUPM-1/$FeCl_3$.

Band Position (cm-1)	Band Assignments & Description
3431 (br)	N-H stretch from both pyrrole & benzenediamine moieties overlap with O-H stretch of terminal groups
3267 (w)	Can be assigned to NH_2 stretches of 1,4-benzenediamine moiety
2927 (m)	Aliphatic C-H stretch of CH_2 linkage, NOT present in neither benzenediamine nor pyrrole monomers
1612 (m)	Aromatic C=C vibration mode for the Asymmetric aromatic rings in the copolymer
1512 (w)	Phenyl ring C=C vibration mode, characteristic band, proves the presence of the benzenediamine moiety in the copolymer
1433 (w)	Can be assigned to the phenyl C=C vibrational mode
1120 (w)	C-N stretch in both the benzenediamine and pyrrole moieties in the polymer
673 (m)	NH_2 wagging

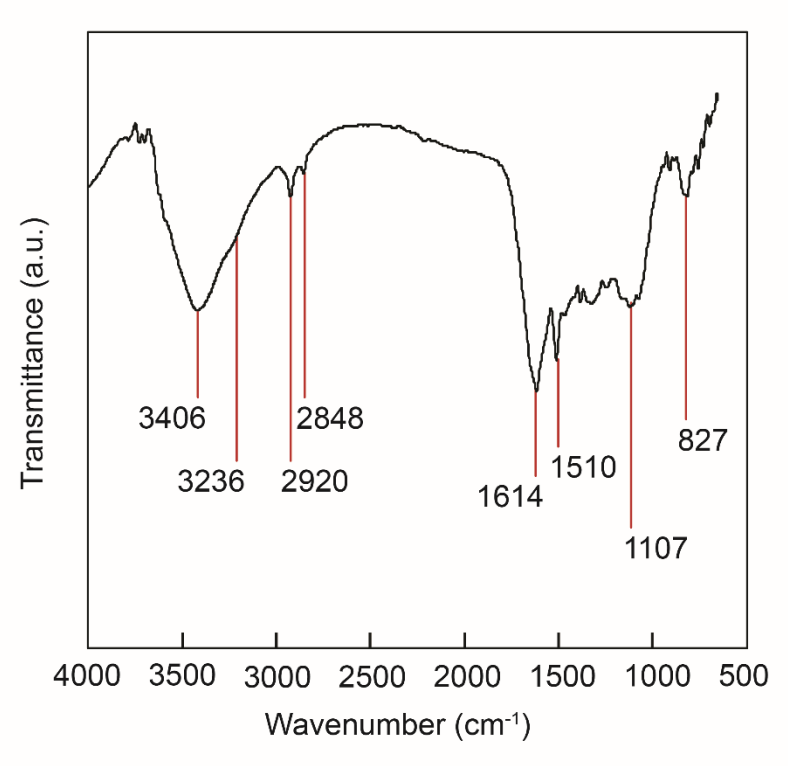

Figure S8. FT-IR spectrum of KFUPM-1/CuCl.

Table S8. Assignment of the FT-IR spectrum peaks of the synthesized KFUPM-1/CuCl.

Band Position (cm^{-1})	Band Assignments & Description
3406 (br)	N-H stretch for the pyrrole as well as the benzenediamine moieties overlap with O-H stretch, terminal OH
3236 (w)	Can be assigned to NH_2 group for the 1,4-benzenediamine moieties.
2920 (w)	Aliphatic C-H stretch of CH_2 linkage, NOT present in neither benzenediamine nor pyrrole monomers
1614 (m)	Aromatic C=C vibration mode for the Asymmetric aromatic rings in the copolymer and phenyl ring C=C vibration mode
1423 (w)	Can be assigned to the phenyl C=C vibrational mode
1107 (w)	C-N stretch in both the benzenediamine and pyrrole moieties in the polymer
827 (w)	NH_2 wagging

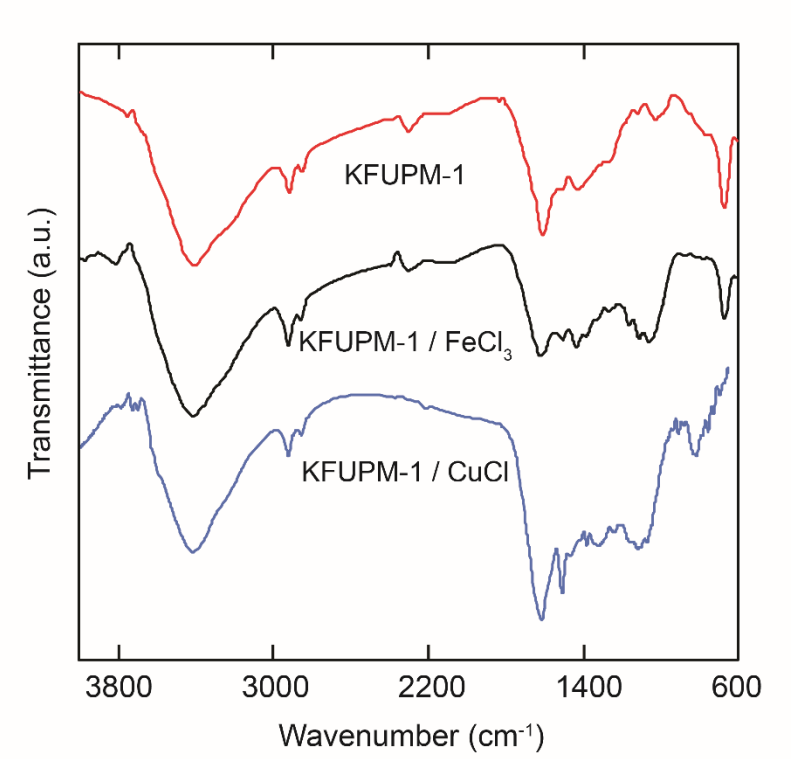

Figure S9. Stack mode of the FT-IR spectra of the polymers KFUPM-1 (red), KFUPM-1/$FeCl_3$ (black), and KFUPM-1/CuCl (blue).

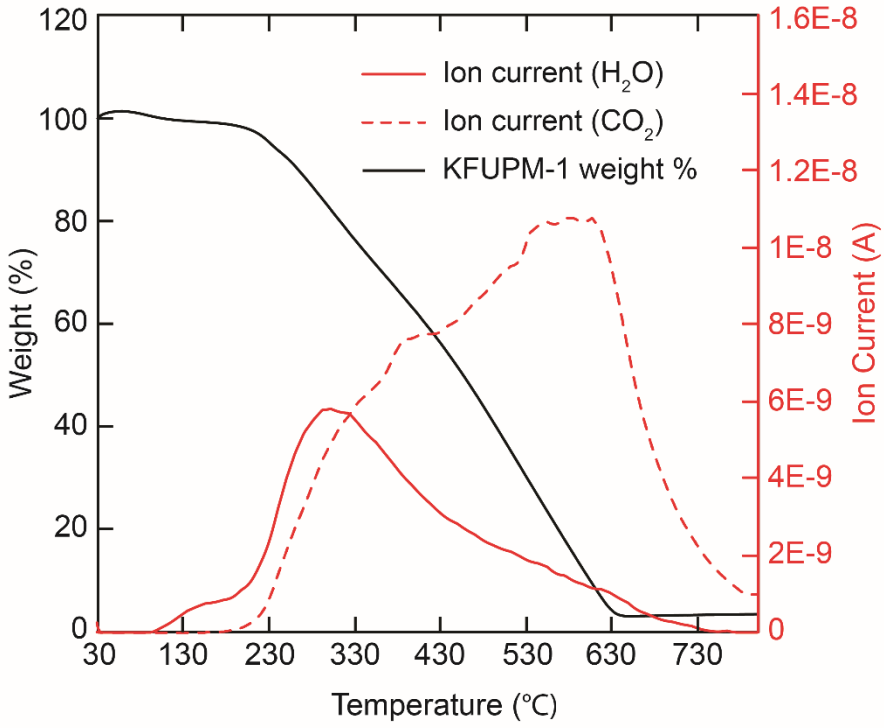

Figure S10. TGA-MS of the KFUPM-1 activated sample under air, the solid red line represents the H_2O molecules emitted from the sample, while the dashed red line represents the CO_2.

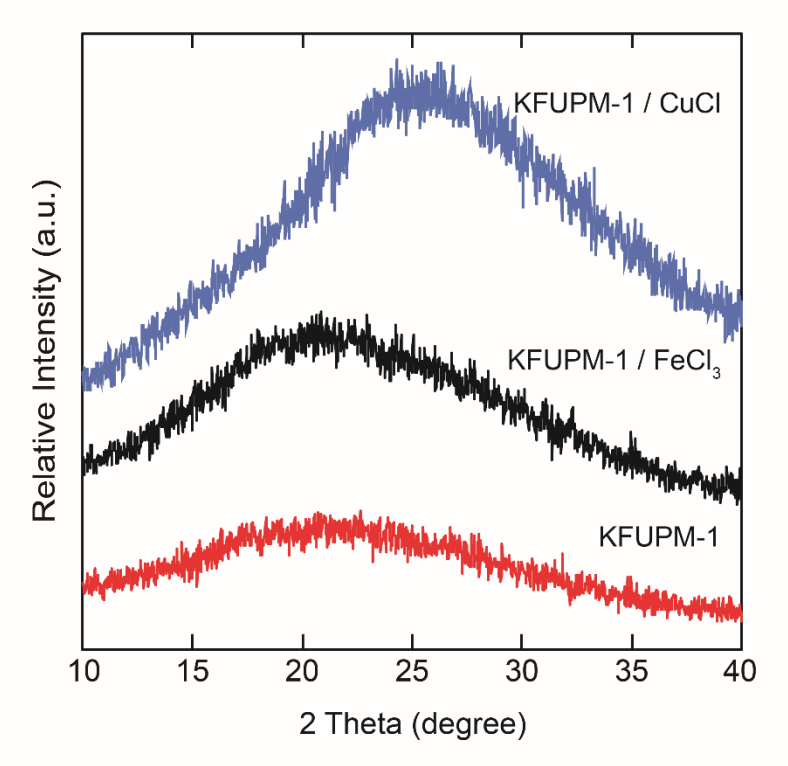

Figure S11. Powder X-ray diffraction of KFUPM-1 (red), KFUPM-1/$FeCl_3$ (black) and KFUPM-1/CuCl (blue).

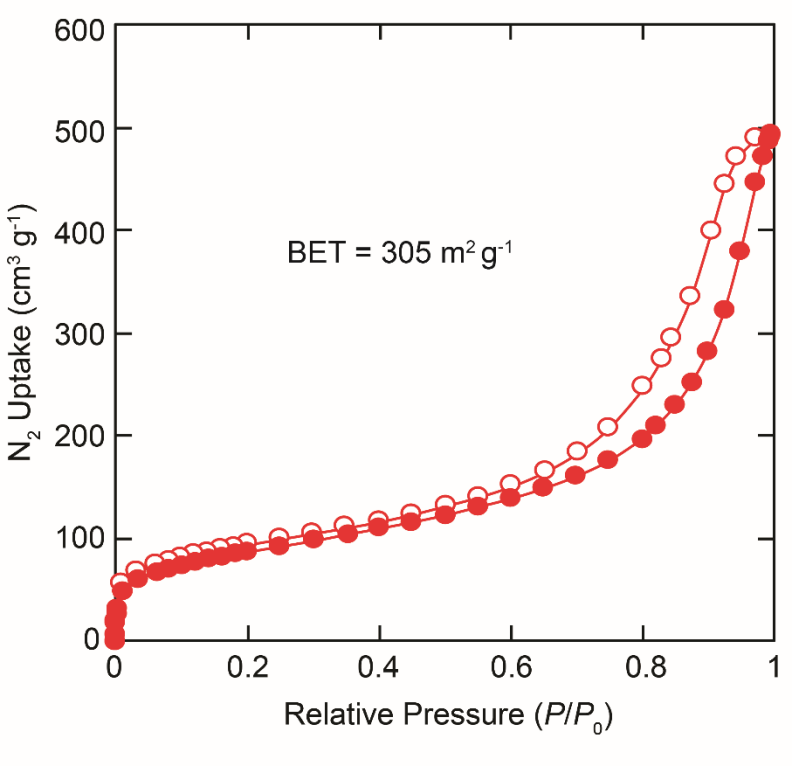

Figure S12. N_2 adsorption isotherm at 77 K. Filled and open symbols represent adsorption and desorption branches, respectively. The connecting lines serve as guides for the eye.

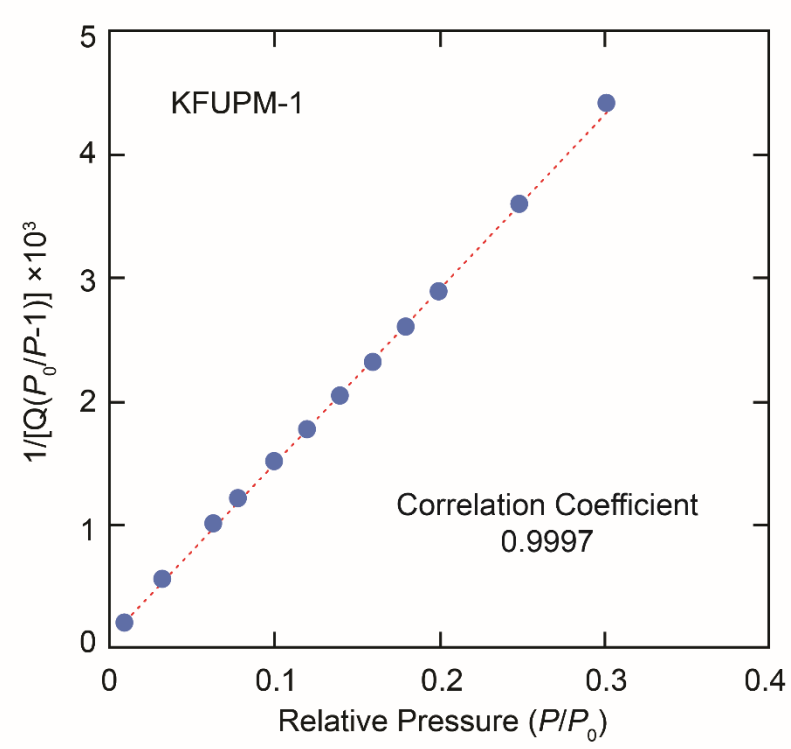

Figure S13. BET plot of KFUPM-1 from experimental N_2 isotherm at 77 K within low relative pressure showing data points (blue circles) and the trend line (red dashed line).

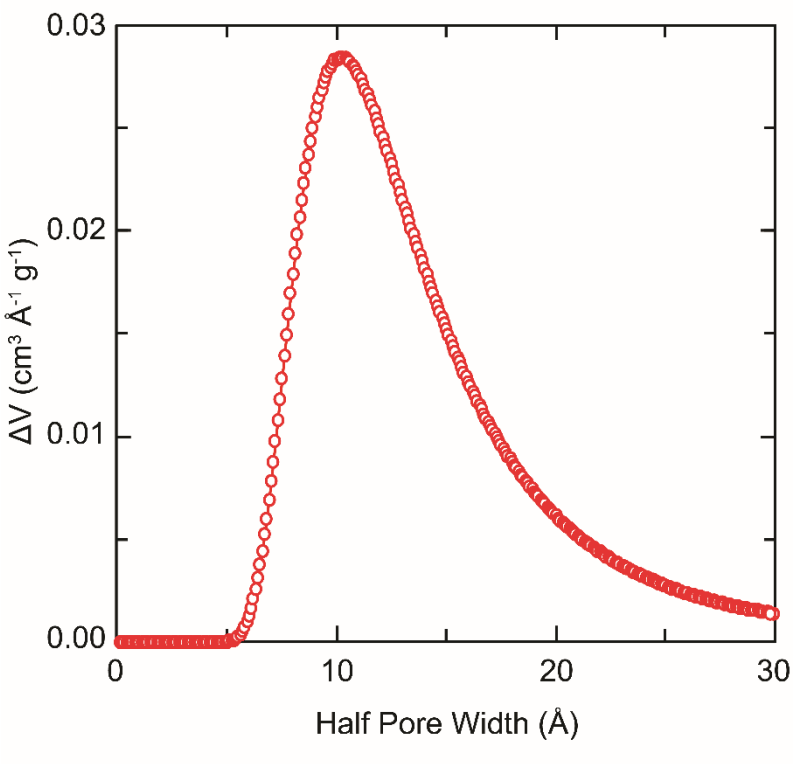

Figure S14. Differential pore size distribution as calculated by Dubinin-Astakhov (DA) method.

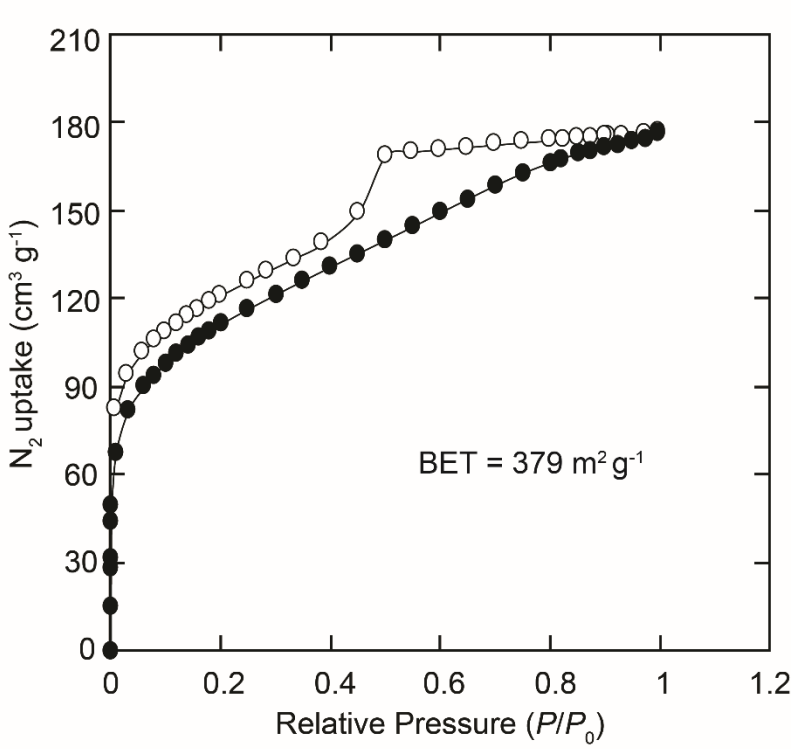

Figure S15. N_2 adsorption isotherm at 77 K for KFUPM-1/$FeCl_3$. Filled and open symbols represent adsorption and desorption branches, respectively. The connecting lines serve as a guide to the eye.

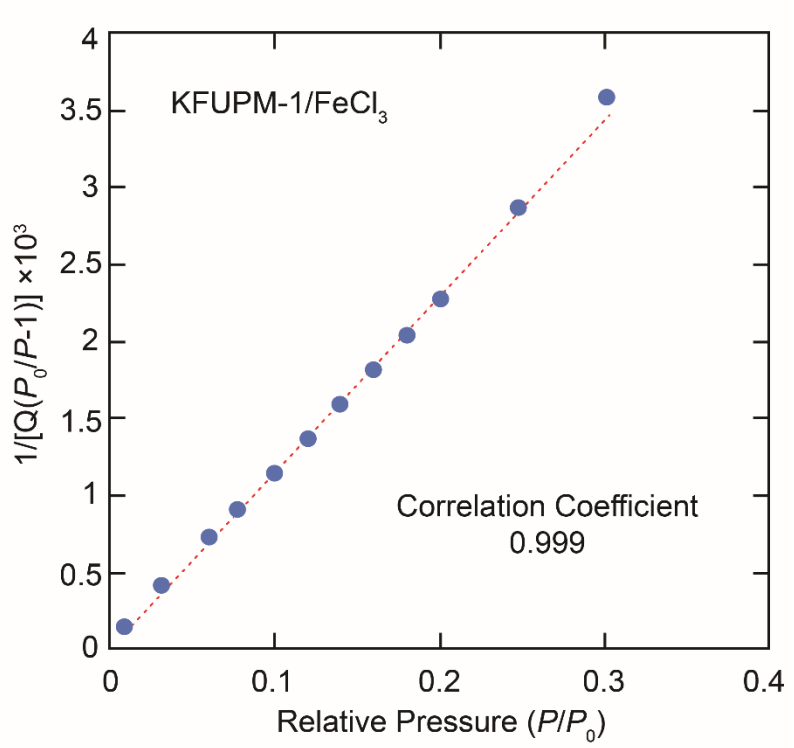

Figure S16. BET plot of KFUPM-1/$FeCl_3$ from experimental nitrogen adsorption isotherm at 77 K within low relative pressure showing data points (blue circle), and the trend line (red dashed line).

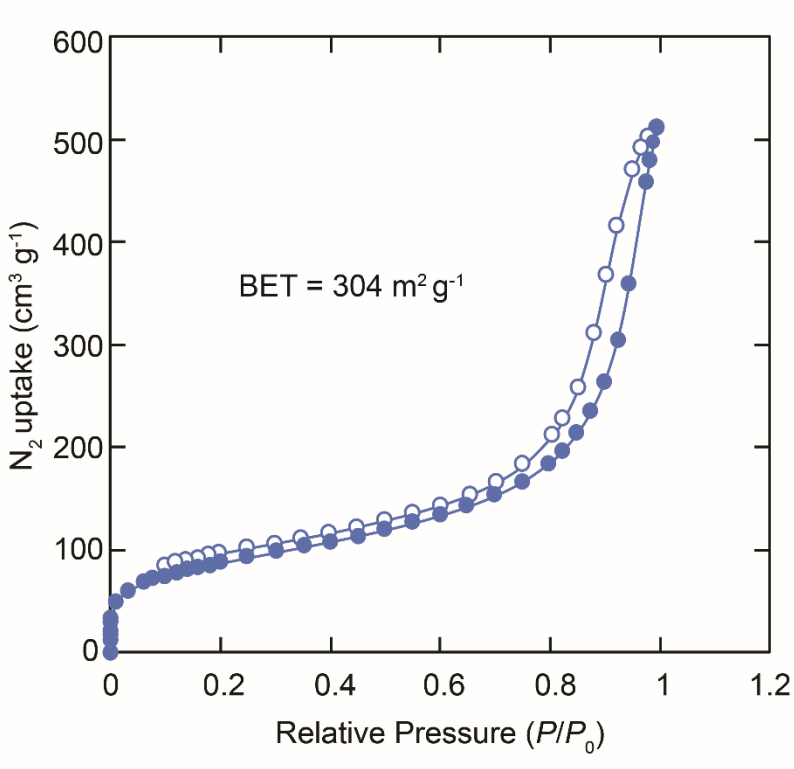

Figure S17. N_2 adsorption isotherm at 77 K for KFUPM-1/CuCl. Filled and open symbols represent adsorption and desorption branches, respectively. The connecting lines serve as a guide to the eye.

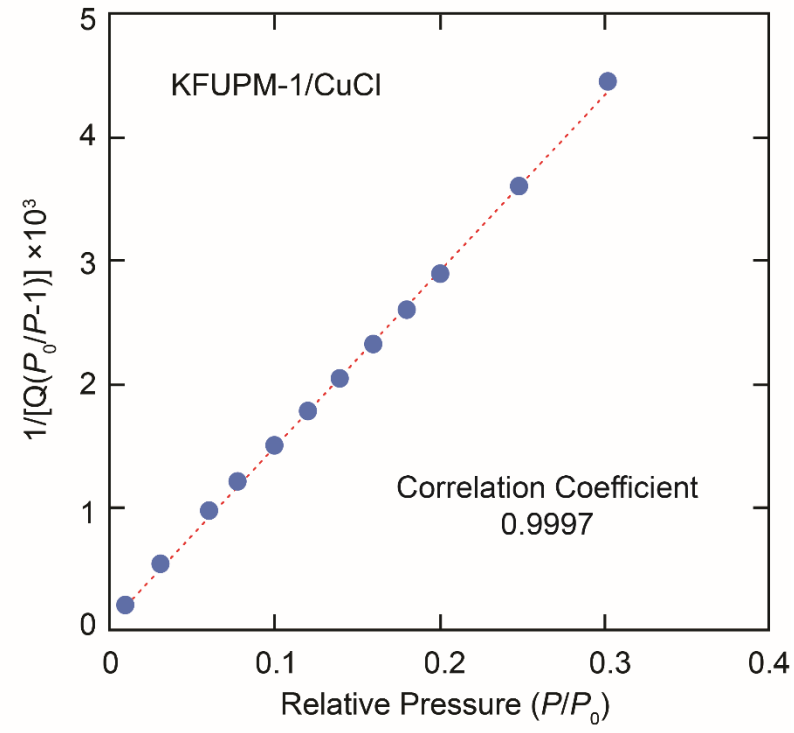

Figure S18. BET plot of KFUPM-1/CuCl from experimental nitrogen adsorption isotherm at 77 K within low relative pressure showing data points (blue circle), and the trend line (red dashed line).

Section S4: Gas Adsorption Studies

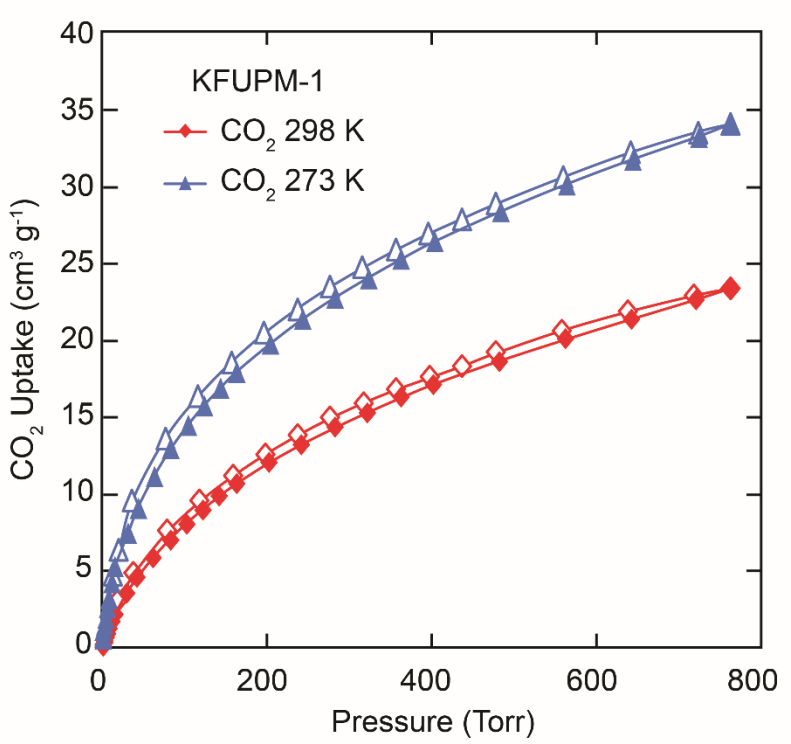

Figure S19. CO_2 sorption isotherms for KFUPM-1 at 273 K (triangle) and 298 K (diamond). Filled and open symbols represent adsorption and desorption branches, respectively. The connecting lines serve as a guide to the eye.

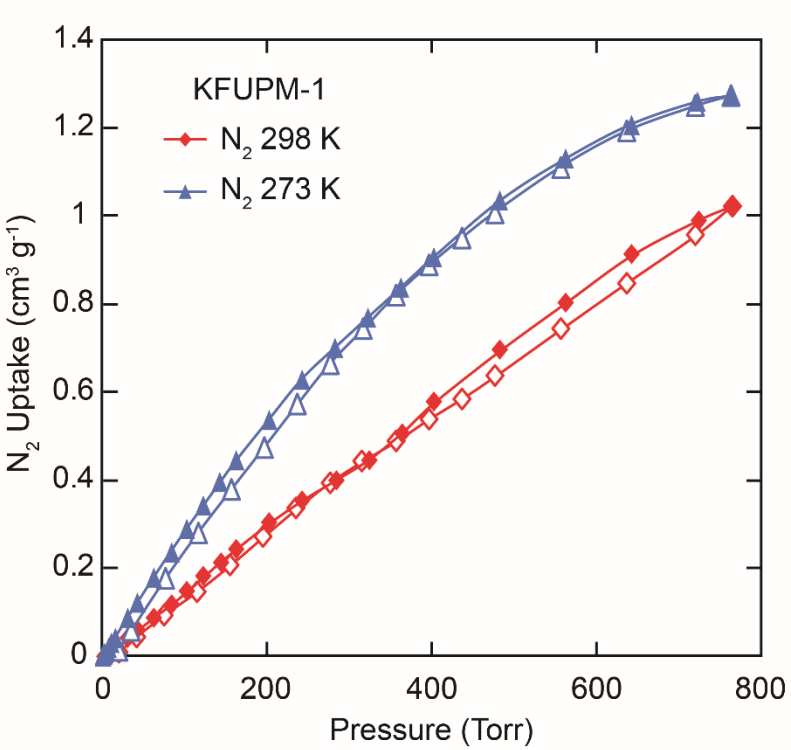

Figure S20. N_2 sorption isotherms for KFUPM-1 at 273 K (triangle) and 298 K (diamond). Filled and open symbols represent adsorption and desorption branches, respectively. The connecting lines serve as a guide to the eye.

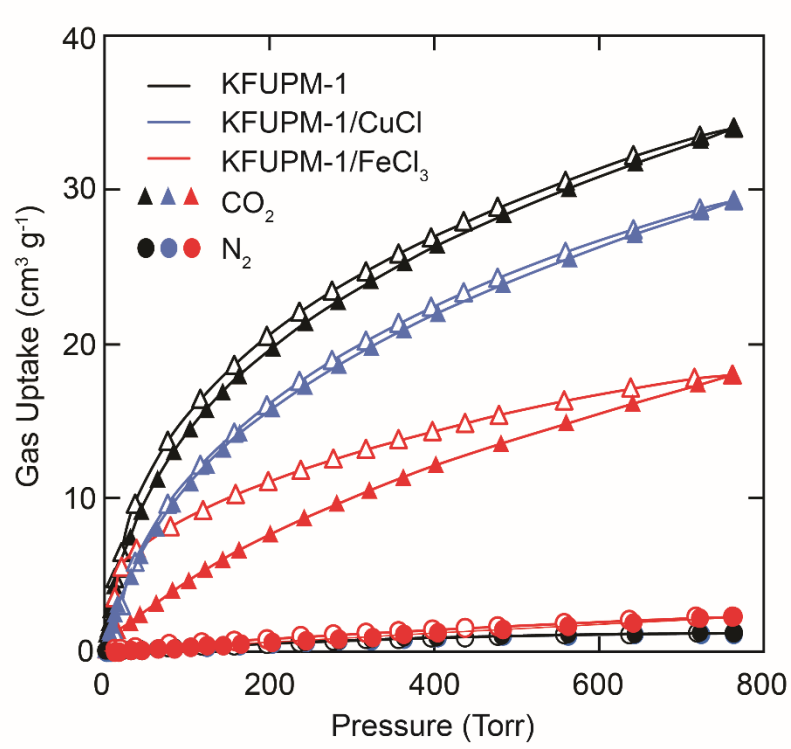

Figure S21. CO_2 (triangle) and N_2 (circle) sorption isotherms for KFUPM-1 (black), KFUPM-1/CuCl (blue), and KFUPM-1/$FeCl_3$ (red) at 273 K. Filled and open symbols represent adsorption and desorption branches, respectively. The connecting lines serve as a guide to the eye.

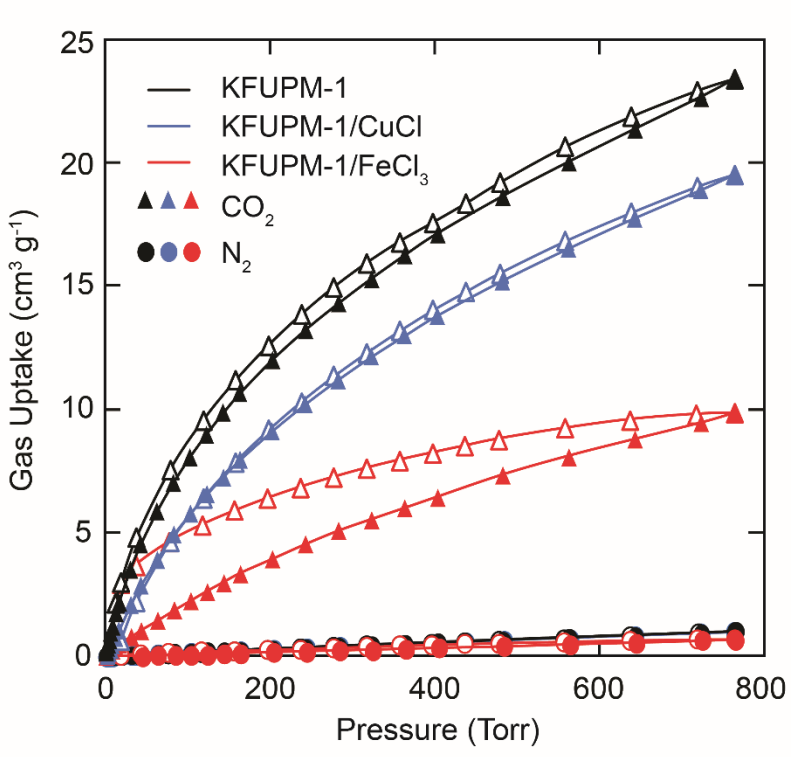

Figure S22. CO_2 (triangle) and N_2 (circle) sorption isotherms for KFUPM-1 (black), KFUPM-1/CuCl (blue), and KFUPM-1/$FeCl_3$ (red) at 298 K. Filled and open symbols represent adsorption and desorption branches, respectively. The connecting lines serve as a guide to the eye.

Coverage Dependent Enthalpy of Adsorption (Q_{st})

The Q_{st} estimates the affinity of specific gas molecules and adsorbent material. This property is intrinsic for a material and independent of the temperature. A virial-type expression comprising temperature independent parameters a_i and b_j was used in order to relate between two different single component isotherms of CO_2 gas at two different temperatures (273 K and 298 K). The virial-type equation used is: [1]

$$\mathrm{Ln}(p) = \ln(v) + \frac{1}{T}\sum_{i=0}^{m}(a_i\, v_i) + \sum_{i=0}^{n}(b_i\, v_i) \qquad (1)$$

where, P is pressure (Pa), v is the adsorbed amount (mol/g), a_i and b_j are the virial coefficient, T is temperature, and m and n represent the number of coefficients required to describe the isotherms, the iteration will be applied until reach the minimum values of theses constants.

Henry's Law Selectivity

The selectivity of the synthesized polymer (KFUPM-1) toward CO_2 and CH_4 is estimated using Henry's model, since it describes the gas adsorption on solid as linear relation. The Henry's isotherm equation is: [2]

$$q = kP \qquad (2)$$

where, q is the adsorbed amount of gas per unit weight of the material (cc/g), P is the adsorbate gas pressure (torr), and k is the Henry's law constant (cc/g.torr).

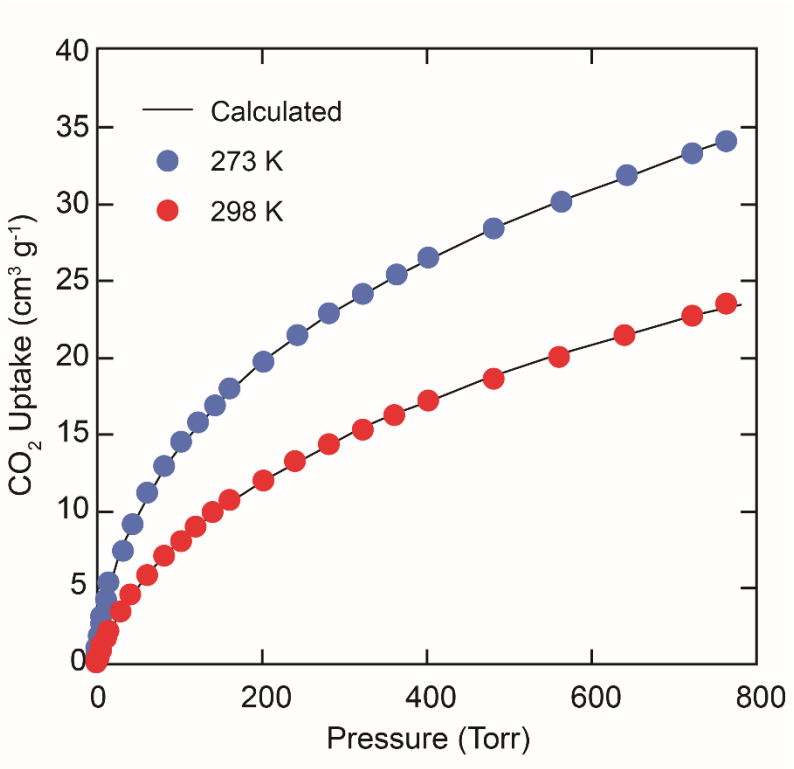

Figure S23. Virial-type equation fitting (black line) of experimental CO_2 adsorption data for KFUPM-1 at 273 K (blue circle) and 298 K (red circle).

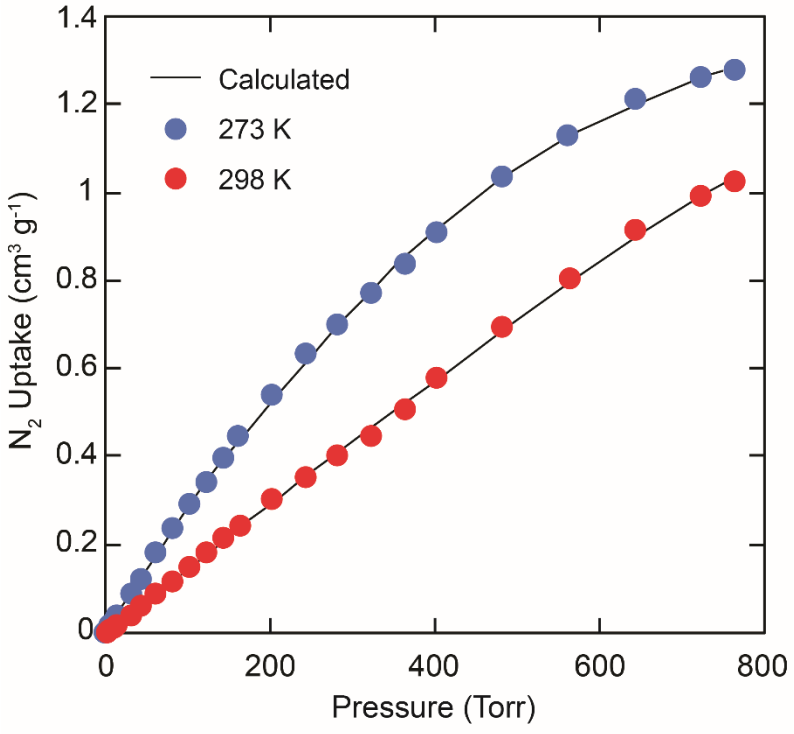

Figure S24. Virial-type equation fitting (black line) of experimental N_2 adsorption data for KFUPM-1 at 273 K (blue circle) and 298 K (red circle).

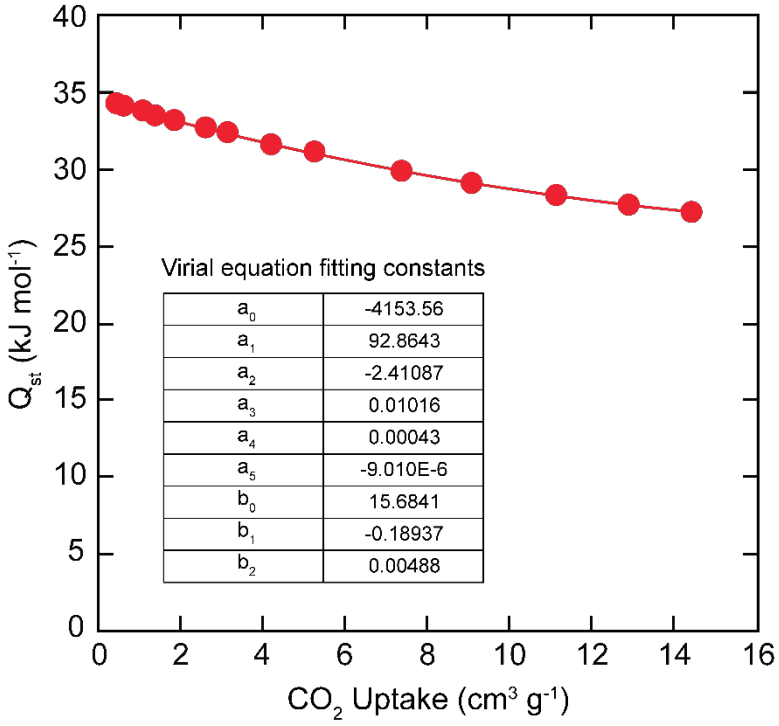

Figure S25. Calculated enthalpy of adsorption (Q_{st}) of CO_2 gas for KFUPM-1. Inset provides the constants used for the fitting of 273 K and 298 K CO_2 adsorption isotherms using virial-type equation.

Calculation of CO_2/N_2 IAST Selectivity

The Ideal Adsorbed Solution Theory (IAST) is used to calculate the composition of the adsorbed phase from pure component isotherms and predicting the selectivity of the binary mixture CO_2/N_2.

IAST assumes an ideal behaviour to represent the relationship between the bulk gas phase and adsorbed phase as:

$$y_i\, P_t = x_i\, P_i \quad (3)$$

where P_t is the total pressure of gas mixture in the bulk phase, P_i is the standard state pressure of pure component *i* which yields the same spreading pressure as that of the mixture at the same temperature, y is the molar fraction of the bulk phase, and *x* is the molar fraction of the adsorbed phase.

For two components (a and b), the equilibrium obtained from the spreading pressure results in:

$$\int_0^{P_a} \frac{q_a}{P}\, dP = \int_0^{P_b} \frac{q_b}{P}\, dP \quad (4)$$

Combining Eq. (3) and (4) resulting in:

$$\int_0^{\frac{y_a P_t}{x_a}} \frac{q_b}{P}\, dP = \int_0^{\frac{y_b P_t}{x_b}} \frac{q_b}{P}\, dP \quad (5)$$

The molar fraction of a mixture should be unity.

$$y_a + y_b = 1 \quad (6)$$

$$x_a + x_b = 1 \quad (7)$$

Here, q_a and q_b are the adsorption isotherms of components a and b; they can be fitted from experimental data by using dual-site Langmuir method as:

$$q_i = \frac{q_{max1,i}\ K1_i\ y_i\ P_t}{1+K1_i\ y_i\ P_t} + \frac{q_{max2,i}\ K2_i\ y_i\ P_t}{1+K2_i\ y_i\ P_t} \quad (8)$$

where $q_{max1,i}$ and $q_{max2,i}$ are the saturation capacities of component *i* (a or b) and *K1* and *K2* are the affinity constants.

Given P_t, *y*, q_{max} and *K* , there is only one unknown variable quantity *x* which can be solved by MATLAB software. The selectivity can, then, be estimated as:

$$S = \frac{x_a/y_a}{x_b/y_b} \quad (9)$$

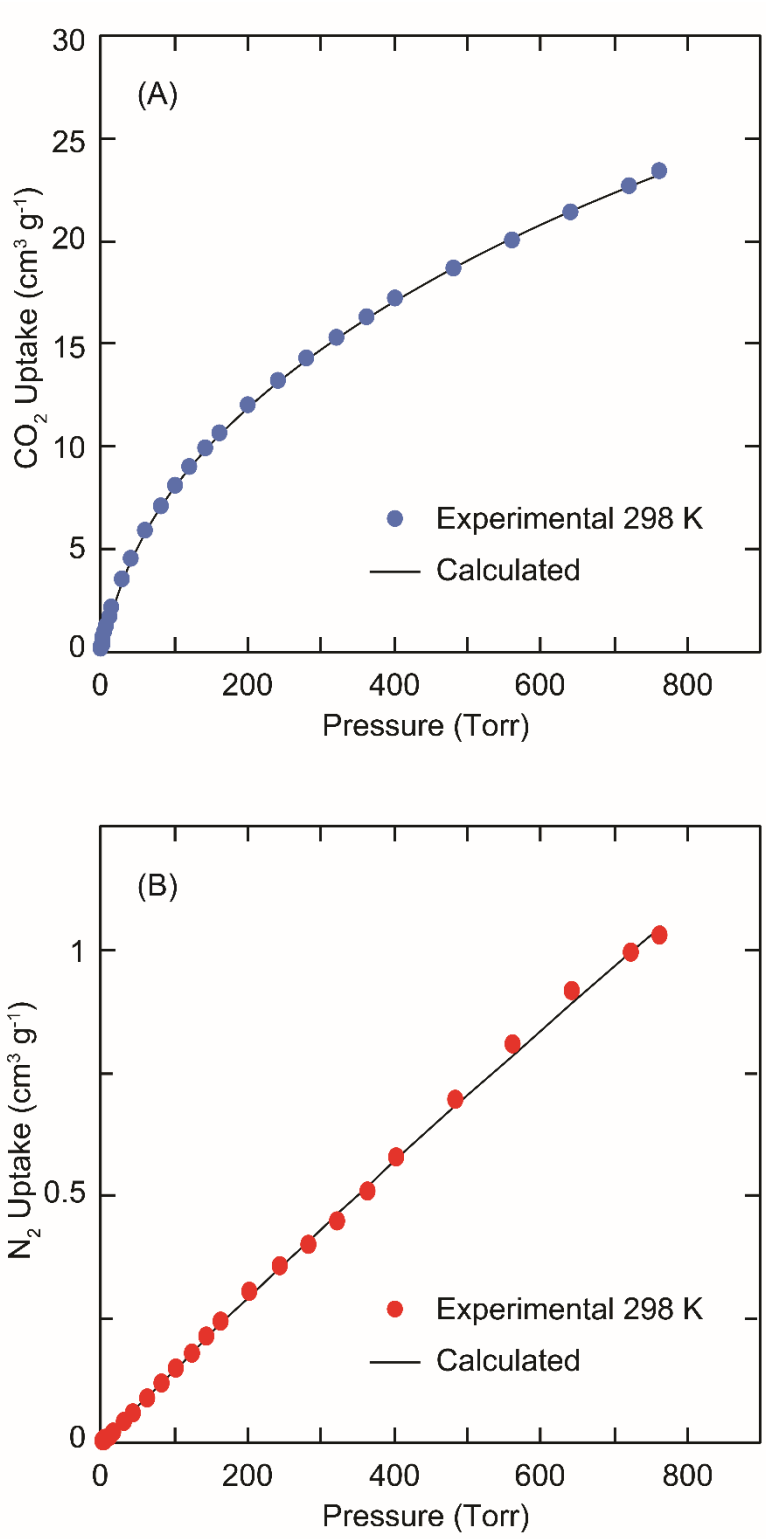

Figure S26. Dual-site Langmuir fitting of experimental isotherms at 298 K for (A) CO_2 (blue circle), and (B) N_2 (red circle).

Table S9. Dual site Langmuir fitting parameters for CO_2 and N_2 adsorption at 298K for KFUPM-1.

CO_2		N_2	
$qmax_1$	8.4790391724590	$qmax_1$	10.1700610532542
K_1	0.0146335714423	K_1	0.0001509288138
$qmax_2$	42.4294292028068	$qmax_2$	-0.0066302405165
K_2	0.0007526233526	K_2	-30.0495872907169

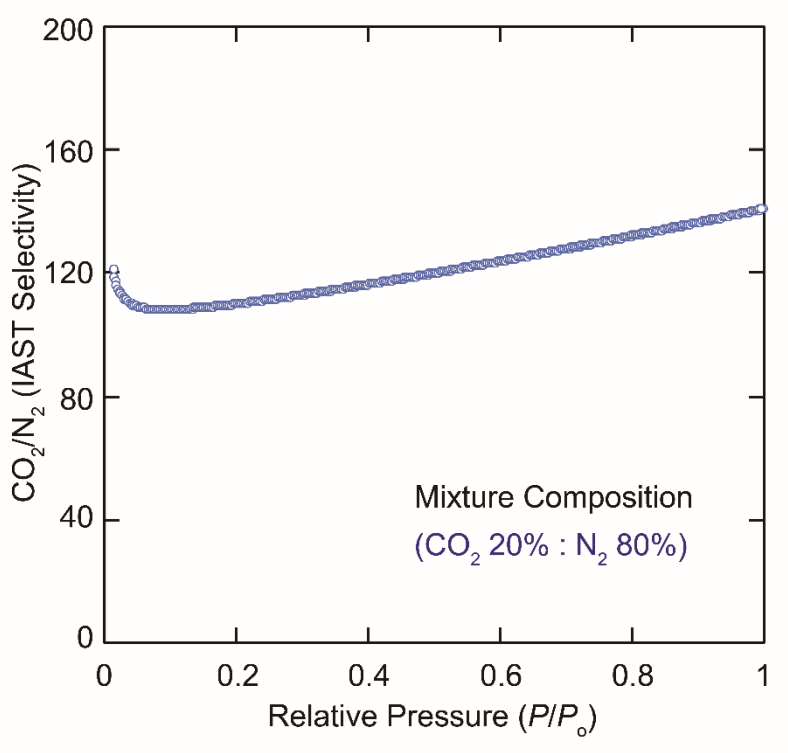

Figure S27. Ideal Adsorption Solution Theory (IAST) selectivity of CO_2/N_2 at 298 K for KFUPM-1.

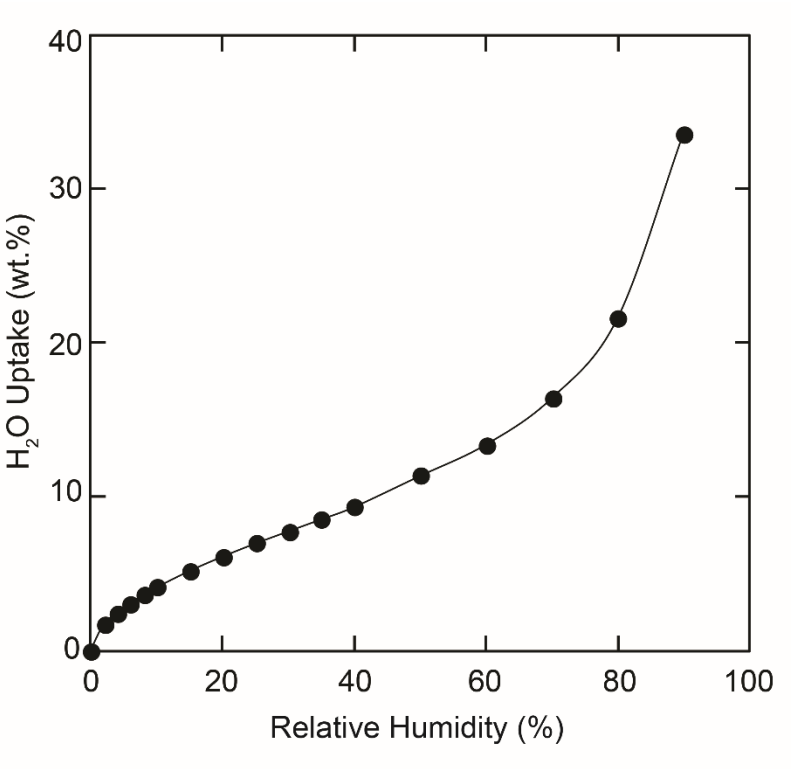

Figure S28. Water isotherm of KFUPM-1 at 298 K.

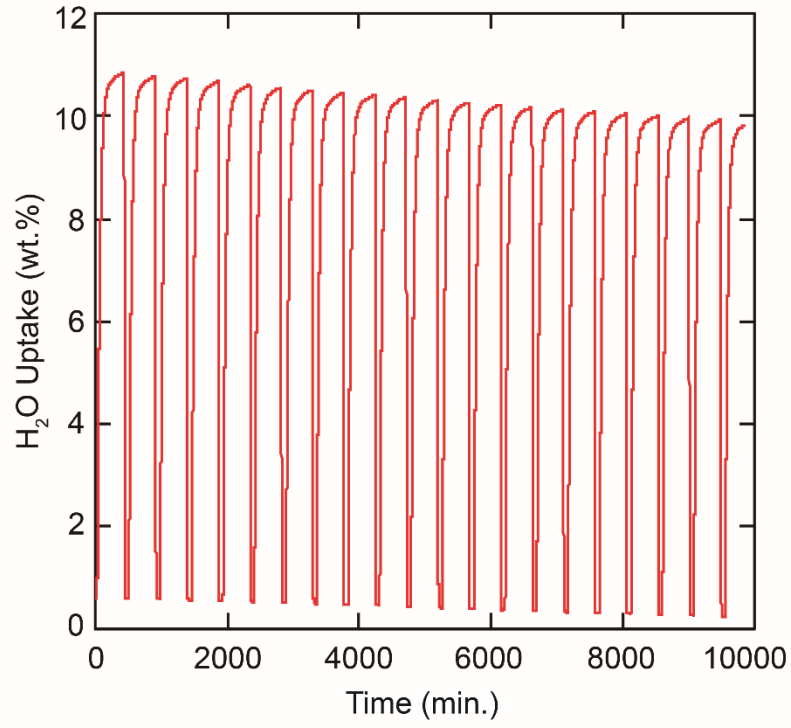

Figure S29. Water adsorption cycles at 313 K and 76% RH. Activation between cycles was carried out at 383 K under vacuum.

Section S5. Breakthrough Experiments

A dynamic $CO_2/N_2/H_2O$ breakthrough setup was constructed to separate CO_2 from a $CO_2/N_2/H_2O$ mixture (representing a flue gas) as shown in Figure S28. The home-made system is composed of a fixed adsorbent bed column (Inner diameter = 4 mm, Outer diameter = 6 mm and Length = 20 cm) which is filled with the KFUPM-1 sample (1.12 g), CO_2 and N_2 cylinders, H_2O humidifier, two gas regulators with dual pressure gauges and output control valves, two mass flow controllers (one calibrated for CO_2 flow and the other calibrated for N_2), two check valves, bypass line (for calibrating the mass spectrometer from the input feed gas), bourdon absolute pressure, mass spectrometer (to analyze the output concentration of effluent gases from the bed), heater jacket and vacuum pump (for regeneration purpose), and interconnecting stainless steel valves and tubes to control and regulate the flow of carrier gas within the system.

The first step in the operation of breakthrough setup involves the degassing of the sample at 373 K under vacuum for 24 hours to remove any guest molecules trapped inside the pores of KFUPM-1. The breakthrough experiments were conducted under ambient conditions (298 K and 1 bar). The flow rate of the feed gas which was a mixture of 20% CO_2 and 80% N_2 was kept constant at 10 sccm. For the humid mixture, the gases (20% CO_2 and 80% N_2) were wet by passing through a water humidifier. In order to control the relative humidity, we first pass dry N_2 gas through a water humidifier at a constant flow rate (10 sccm) and at constant temperature (298 K) until H_2O percentage reaches equilibrium in the mass spectrometer. This condition generating ~2.73% (vol/vol) of moisture, which is equivalent to 91% relative humidity. The full breakthrough capacity of CO_2 and N_2 was measured by evaluating the ratio of compositions of the downstream gas and the feed gas.

The CO_2 adsorption capacity of the KFUPM-1 is evaluated using the expression. [3]

$$q_{co_2} = \frac{1}{m} F\ C\ t \qquad (10)$$

where q_{co_2} represents the CO_2 capacity, m mass of adsorbent (g), F is the input flow rate (cm^3min^{-1}), C is influent CO_2 concentrations (vol.%), t is the time (min).

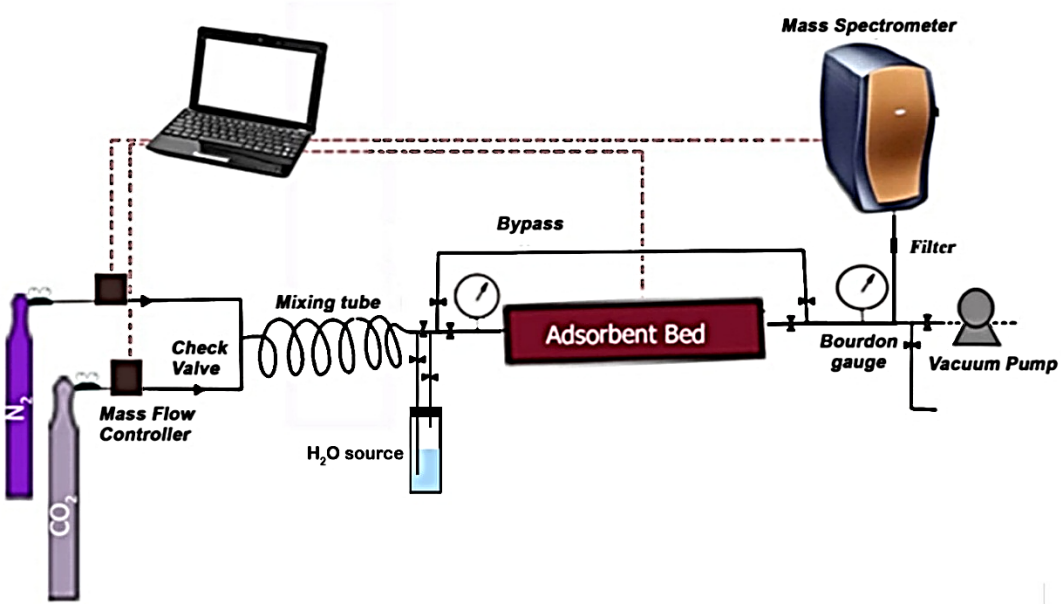

Figure S30. Schematic diagram of $CO_2/N_2/H_2O$ adsorption breakthrough setup.

Section S6. References

1. Czepirski and J. JagieŁŁo, *Chem. Eng. Sci*., 1989, **44**, 797–801.
2. S.-C. Xiang, Z. Zhang, C.-G. Zhao, K. Hong, X. Zhao, D.-R. Ding, M.-H. Xie, C.-D. Wu, M. C. Das, R. Gill, K. M. Thomas and B. Chen, *Nat. Commun*., 2011, 2, 204.
3. P. Nugent, Y. Belmabkhout, S. D. Burd, A. J. Cairns, R. Luebke, K. Forrest, T. Pham, S. Ma, B. Space, L. Wojtas, M. Eddaoudi and M. J. Zaworotko, *Nature*, 2013, **495**, 80–84.
4. R. J. Li, M. Li, X. P. Zhou, D. Li, M. O'Keeffe, *Chem. Commun*., 2014, **50**, 4047–4049.